Atmos. Chem. Phys. Discuss., 9, 17385–17427, 2009
www.atmos-chem-phys-discuss.net/9/17385/2009/

Atmospheric Chemistry and Physics Discussions

This discussion paper is/has been under review for the journal *Atmospheric Chemistry and Physics (ACP)*. Please refer to the corresponding final paper in *ACP* if available.

Cross-hemispheric transport of central African biomass burning pollutants: implications for downwind ozone production

E. Real[1,*], E. Orlandi[2], K. S. Law[1], F. Fierli[2], D. Josset[1], F. Cairo[3], H. Schlager[5], S. Borrmann[4a,b], D. Kunkel[4a], M. Volk[6], J. B. McQuaid[7], D. J. Stewart[8], J. Lee[9], A. Lewis[9], J. R. Hopkins[10], F. Ravegnani[11], A. Ulanovski[12], and C. Liousse[13]

[1]LATMOS-Service d'Aéronomie/UPMC/UVSQ/IPSL, CNRS-INSU, 4 Place Jussieu, 75252, Paris, France
[2]ISAC-CNR Bologna, Italy
[3]Instituto di Scienze dell'Atmosfera e del Clima, Roma, Italy

[4a] Max Planck Institute for Chemistry, Particle Chemistry Dept., Germany
[4b] Institute for Atmospheric Physics, Johannes Gutenberg University, Mainz, Germany
[5] Deutsches Zentrum für Luft- und Raumfahrt (DLR), Oberpfaffenhofen, Institut für Physik der Atmosphäre, 82230 Wessling, Germany
[6] Institut für Meteorologie und Geophysik, Universität Frankfurt, Frankfurt, Germany
[7] Institute for Climate and Atmospheric Science School of Earth and Environment, University of Leeds, UK
[8] Dept. of Chemistry, University of Reading, Reading, UK
[9] National Centre for Atmospheric Science Dept. of Chemistry, University of York, York, UK
[10] National Centre for Atmospheric Science, University of York, York, UK
[11] Institute of Atmospheric Sciences and Climate, CNR, Bologna, Italy
[12] CAO, Dolgoprudny, Russia
[13] Laboratoire d'Aérologie, Université de Toulouse, France
[*] now at: CEREA, ENPC/EDF, 20 rue Alfred Nobel 77455 - Champs sur Marne, France

Received: 4 May 2009 – Accepted: 21 May 2009 – Published: 20 August 2009

Correspondence to: E. Real (elsa.real@aero.jussieu.fr)

Published by Copernicus Publications on behalf of the European Geosciences Union.

Abstract

Pollutant plumes with enhanced levels of trace gases and aerosols were observed over the southern coast of West Africa during August 2006 as part of the AMMA wet season field campaign. Plumes were observed both in the mid and upper troposphere. In this study we examined both the origin of these pollutant plumes and their potential to produce O_3 downwind over the Atlantic Ocean. Runs using the BOLAM mesoscale model including biomass burning CO tracers were used to confirm an origin from central African fires. The plumes in the mid troposphere had significantly higher pollutant concentrations due to the fact that transport occurred from a region nearer or even over the fire region. In contrast, plumes transported into the upper troposphere over West Africa had been transported to the north-east of the fire region before being uplifted. Modelled tracer results showed that pollutants resided for between 9 and 12 days over Central Africa before being transported for 4 days, in the case of the mid-troposphere plume and 2 days in the case of the upper tropospheric plume to the measurement location over the southern part of West Africa. Around 35% of the biomass burning tracer was transported into the upper troposphere compared to that remaining in the mid troposphere. Runs using a photochemical trajectory model, CiTTyCAT, were used to estimate the net photochemical O_3 production potential of these plumes. The mid tropospheric plume was still very photochemically active (up to 7 ppbv/day) especially during the first few days of transport westward over the Atlantic Ocean. The upper tropospheric plume was also still photochemically active, although at a slower rate (1–2 ppbv/day). Trajectories show this plume being recirculated around an upper tropospheric anticyclone back towards the African continent (around 20° S). The potential of theses plumes to produce O_3 supports the hypothesis that biomass burning pollutants are contributing to the observed O_3 maxima over the southern Atlantic at this time of year.

ACPD

9, 17385–17427, 2009

1 Introduction

Biomass burning produces large amounts of pollutants which can be transported many thousands of kilometres downwind. This includes trace gases such as CO_2, and precursors to O_3 as well as aerosols which can also have an important impact on radiative forcing. Production of O_3 downwind from source regions also influences the global oxidizing capacity through the formation of the OH radical, and thus the lifetime of greenhouse gases such as CH_4. Africa emits the largest amount of biomass burning (BB) emissions with a strong interhemispheric transition between West Africa in boreal winter to Central and Southern Africa in boreal summer (Crutzen and Andreae, 1990) following the location of the dry season in each hemisphere.

Long-range transport of BB out of the African continent has been suggested as a source of O_3 over the tropical south Atlantic where enhanced concentrations are found throughtout the year in the mid and upper troposphere, the so-called maximum O_3 pattern (Weller et al., 1996; Thompson et al., 2004; Jenkins and Ryu, 2004a). Cross-hemispheric transport of BB emissions situated in Central Africa during the boreal summer followed by uplift by convective systems and recirculation by the large-scale Hadley cells has been proposed to explain this phenomenon (Jenkins et al., 1997; Sauvage et al., 2005; Mari et al., 2008). Analysis of MOZAIC vertical O_3 profiles collected over the southern coast of West Africa attributed around 30% of mid-tropospheric O_3 enhancements to cross-hemispheric transport of BB emissions from Central Africa during boreal summer (Sauvage et al., 2005). More recent CO profile data collected by MOZAIC aircraft over Lagos also show higher concentrations during June-July-August (JJA) (Sauvage et al., 2006) although local anthropogenic sources could also contribute. These air masses are then available for uplift by deep convection associated with the summer monsoon into the upper troposphere (Mari et al., 2008).

Uplift of O_3 and its precursors from local anthropogenic sources, cross-hemispheric BB sources or as a result of lightning NO_x (LiNOx) emissions associated with deep convection can contribute to observed upper level O_3 and CO maxima. Previous studies

ACPD
9, 17385–17427, 2009

have suggested an important role for LiNOx in particular (Jacob et al., 1996; Jenkins and Ryu, 2004b; Sauvage et al., 2007). Uplift of pollution over Asia in the monsoon followed by long-range transport in the tropical tropopause layer (TTL) could also explain CO and O_3 maxima in the upper troposphere (Barret et al., 2008).

The relative importance of mid-level versus upper level transport of BB emissions from Central Africa requires further quantification together with the O_3 production potential of these air masses over West Africa and downwind over the southern Atlantic Ocean and their contribution to observed O_3 maxima. Previous studies of quantifying O_3 production in plumes focused on BB emissions from southern Africa where O_3 was produced mainly over the continents with smaller net production during long-range transport over the ocean ranging from negative to positive depending on the study and whether lightning emissions were taken into account (e.g. Mauzerall et al., 1998; Chatfield et al., 1996; Thompson et al., 2004).

In this paper, we examine the origin and O_3 production potential of two pollution plumes observed in the mid troposphere (MT) and upper troposphere (UT) during August 2006 over the southern coast of West Africa during the AMMA (African Monsoon Multidisciplinary Analysis) project. Based on back trajectory calculations, these plumes appear to originate from central African BB regions (Law et al., in preparation, 2009) (Andres-Hernandez et al., 2009). The plume observations are discussed in Sect. 2. Their origin and transport pathways to West Africa are investigated using fire CO tracers run in a mesoscale model (Sect. 3). The results from these simulations are used to understand the mechanisms responsible for transporting the plumes from the Southern to the Northern Hemisphere where they were observed in the MT and UT. Travel times between the source region and the observations as well as the fraction of tracer in the UT compared to the MT are also estimated. We then investigate the O_3 production potential in both the MT and UT plumes during transport downwind from West Africa over the Atlantic Ocean using simulations of a photochemical trajectory model initialised with observations in order to examine their potential to contribute to the summertime O_3 maximum (Sect. 4). Conclusions are presented in Sect. 5.

ACPD
9, 17385–17427, 2009

2 Observational evidence

During August 2006, five aircraft equipped with trace gas and aerosol instrumentation made flights over West Africa as part of an AMMA special observing period with the aim to improve understanding about processes influencing atmospheric composition over this region. An overview of the main findings from this campaign is given in Reeves et al., 2009 including details about instrument payloads and flights. Several flights were made to the southern coast of West Africa over the Gulf of Guinea to look for BB emissions originating from Central Africa. Latitudinal cross sections of O_3 and CO data compiled using all available aircraft data clearly show air masses with enhanced concentrations were sampled in the mid-troposphere (700 to 500 hPa) over the Gulf of Guinea (Reeves et al., in preparation, 2009). Here, we focus on the analysis of plumes observed in the MT and also in the UT on 13 August 2006 when 4 aircraft flew to the south (UK BAe-146 (B-146), French Falcon-20 (FF20), DLR Falcon-20 (DF-20) and the M55-Geophysica (M55)).

First considering the MT plume(s), layers with high concentrations of CO, CO_2, PAN, NO_x, O_3, VOCs and aerosols were sampled between 2.5 and 4.5 km by the B-146, and 3 h later by the DF-20 below 5.5 km (500 hPa) over southern West Africa and the Gulf of Guinea (see Figs. 1, 2, and Table 1). For example, the DF-20 measured up to 450 ppbv CO, 130 ppbv O_3 and more than 8 ppbv NO_y (see Fig. 2). The NO:NO_y was rather low (0.04) indicating that significant photochemical processing had taken place and therefore discounting local anthropogenic emissions as the origin. The FF-20, which flew to the same region, also sampled air masses with elevated CO and O_3 at around 8 km at 6° N on the same day with an origin over the Gulf of Guinea according to Ancellet et al. (2009). The B-146 observed rather similar CO and O_3 concentrations especially in the upper part of their plume sampling suggesting that both aircraft sampled the same polluted air mass. The B-146 also sampled high levels of PAN (greater than 800 pptv) together with high acetonitrile, a strong indicator of BB emissions (Reeves et al., in preparation, 2009). Elevated HCHO and somewhat

ACPD
9, 17385–17427, 2009

enhanced RO2 concentrations were observed in the DF-20 plume with 3-day back trajectories showing air had been transported from the south-east over the Gulf of Guinea Andres-Hernandez et al. (2009). Interestingly, the DF-20 plume also had high CO_2 concentrations up to 390 ppmv (mean value of 387 ppmv). Data collected on the 4 August 2006, when a similar flight was made over this region, also showed evidence for BB plumes with elevated trace gas and aerosol concentrations, including CO_2 up to 379 ppmv Andres-Hernandez et al. (2009). These observations strongly suggest the presence of a large BB plume over the Gulf of Guinea extending between about 3 and 6 km: denoted the MT plume in the rest of the paper.

The high altitude M55 aircraft also flew on this day (see Cairo et al., 2009, for a discussion about the aircraft campaign and payload). Interestingly, a plume was observed by the M55 during a dive over the Gulf of Guinea down to 200 hPa (12 km): denoted the UT plume in the rest of the paper. Observations showed elevated levels of trace gases and aerosols (see Fig. 3). Measurements of CO_2 in the dive (around 380 ppmv) were higher than measured at similar altitudes during the rest of the campaign (see Fig. 3b). Higher CO_2 concentrations in the TTL are usually attributed to uplift of mid-latitude air masses several months earlier when surface concentrations are higher (e.g. Park et al., 2007). However, CO_2 concentrations were also elevated in the BB plume observed by the DF-20 at lower altitudes on the same day. O_3 concentrations were around 60 ppbv which is in the upper range of measurements collected at these altitudes during the rest of the M55 campaign (Reeves et al., in preparation, 2009 and Law et al., in preparation, 2009) and also compared to average tropical profiles reported in Fueglistaler et al. (2009) which show a minimum in the upper troposphere at these altitudes attributed to uplift of O_3-poor air. NO and NO_y were also higher during the plume sampling with up to 300 pptv NO and 1 ppbv NO_y. Whilst, these NO_y levels are not very elevated (Voigt et al., 2008) the fact that the NO:NO_y ratio is around 0.3 suggests that this airmass may also have been influenced by more recent LiNOx emissions associated with deep convection. This point is discussed further in 4.2.

The M55 plume also showed elevated concentrations (up to 1e4 nmol mol−1) of fine-

ACPD
9, 17385–17427, 2009

mode aerosol. Whilst this is in the range of measurements collected at these altitudes during the rest of the campaign Borrmann et al. (2009) the fact that particle mixing ratios for sizes n=6 nm and n=14 nm are very similar indicates that no new nucleation has recently taken place. Analysis of other flights (4 and 11 August) when measurements of the non-volatile fraction are also available show that a significant fraction (up to 60%) of particles in the lower TTL were non-volatile and contained soot or non-volatile organic aerosols suggesting injection from a surface source such as BB emissions could be influencing upper tropospheric aerosol composition over West Africa (Borrmann et al., 2009). Finally, whilst CO was not measured on this day by the M55, the DF-20 and the FF-20 (Ancellet et al., 2009) also sampled plumes with elevated CO at around 11km over the south of West Africa (see Fig. 2). Analysis of MOZAIC data collected between 1 to 16 August 2006 in the upper troposphere also shows the existence of several plumes between the Equator and 5° N with CO concentrations above 150 ppbv and, in one case as high as 230 ppbv in the upper troposphere (240 hPa) (J. P. Cammas., personal communication, 2009) Examination of air mass origins in the TTL (350–380 K, 250 to 50 hPa) for this campaign using ensembles of back trajectories from both the M55 flight paths and the TTL region over West Africa showed that there was a significant influence from air masses originating from Central Africa during the period 10 to 16 August up to 150 hPa (Law et al., 2009).

In summary, it appears that the MT plume(s) has the characteristics of a BB origin whereas the M55 plume sampling may have a double origin and could have been influenced by BB and LiNOx emissions. In the next section we examine the transport mechanisms responsible for transporting these plumes to the MT and UT over West Africa before then evaluating the ozone production potential of these plumes downwind over the Atlantic.

ACPD
9, 17385–17427, 2009

3 Cross-hemispheric transport of BB plumes: mechanisms and travel times

3.1 Meteorological situation

The circulation over West Africa during the summer monsoon is dominated by the northward migration of the Inter-Tropical Front denoting the convergence between south-westerly monsoon winds and north-easterly dry Harmattan winds, and associated westward propagation of organised mesoscale convective systems (MCS) linked to the position and strength of the African Easterly Jet (AEJ). The 2006 monsoon was characterised by slightly higher convective activity (stronger AEJ) than average and an InterTropical Convergence Zone (ITCZ) at 10° N in August. The upper level Tropical Easterly Jet (TEJ), positioned at around 5° N was also stronger in August 2006 with a slight north-east/south-west tilt compared its mean position. For further discussion about the meteorological situation during the wet season in 2006 compared to other years see (Janicot et al., 2008).

As discussed in the Introduction, Sauvage et al. (2006) attributed mid-tropospheric O_3 enhancements over the southern coast of West Africa to direct transport of BB plumes in the mid-troposphere during the summer monsoon. This transport pathway is associated with a convergence zone at 5S over Central Africa followed by transport by south-easterly trade winds over the Gulf of Guinea. Mari et al. (2008) further investigated cross-hemispheric transport of BB pollution during July and August 2006 using of fire tracer simulations in the FLEXPART model. They examined the relationship between the intrusion of BB emissions into West Africa, and the strength of a mid-level jet over Central Africa. This jet previously identified by Burpee (1972); Nicholson and Grist (2003), and denoted African Easterly Jet south (AEJ-S) in Mari et al. (2008) had a mean position around 5° S and 700 hPa in 2006. Mari et al. (2008) found that during so-called AEJ-S active phases (25 July to 2 August 2006; 10 to 31 August 2006), this jet extended westwards over the ocean thus driving lower tropospheric intrusions of BB plumes over the Gulf of Guinea. During break phases (3 to 9 August 2006) such transport is inhibited and BB pollutants remain trapped over the Central African conti-

ACPD
9, 17385–17427, 2009

nent. Whilst Mari et al. (2008) suggested that BB plumes can also be uplifted by deep convection into the upper troposphere followed by westward transport by the TEJ they did not examine this second transport pathway in detail. Here, we use a mesoscale model, BOLAM (Bologna Limited Area Model) Buzzi and Foschini (2000), to examine in more detail the transport mechanisms responsible for transport of central African BB plumes into both the mid and upper over West Africa.

3.2 Model description and simulation set up

BOLAM is a limited-area, primitive equation, terrain-following coordinate, hydrostatic meteorological model. A detailed description of the dynamics and numerical schemes of the model can be found in Malguzzi et al. (2006). The main prognostic variables are the wind components u and v, the potential temperature, the surface pressure, and the specific humidity. The water cycle for stratiform precipitation is described by means of five additional prognostic variables: cloud ice, cloud water, rain, snow, graup. The horizontal discretization is based on a (staggered) Arakawa C grid, in geographical coordinates (latitude-longitude). Deep convection is parameterized using the Kain-Fritsch convection scheme, recently updated on the basis of the revision proposed by Kain (2004).

The model simulations discussed here were run over the domain shown in Fig. 4 and with a horizontal resolution of $0.26^{\circ} \times 0.26^{\circ}$ and 38 hybrid sigma vertical levels from the ground to 10 hPa. The model was initialized using $0.5^{\circ} \times 0.5^{\circ}$ European Centre for Medium Range Weather Forecast (ECMWF) meteorological analyses at 00:00 UT on 15 July 2006 and run for 32 days until 00:00 UT on 16 August 2006. ECMWF analyses were also used to update the lateral boundary conditions every 6 h. Time-varying CO-like BB tracer emissions were introduced into the model for the duration of the run. Daily fire emissions were interpolated from 5-day running-mean averaged emissions taken from the AMMA African BB inventory compiled by Liousse et al. (2009) specifically for 2006. Separate tracers were injected daily for 24 h up to an altitude of 1 km and then transported for the rest of the simulation, in order to follow the fate of

BB plumes emitted each day of the simulation. Figure 5 shows the BB CO emissions averaged between 15 July and 15 August 2006 together with the ECMWF wind field at 750 hPa averaged over the same period. The two possible transport pathways of BB plumes in lower troposphere to the north-east and north-west can be seen.

3.3 BB tracer results: UT versus MT transport pathways

The performance of the BOLAM model in reproducing convective activity was evaluated using cloud top brightness temperatures (CTBTs) derived from the 10.8 micrometers channel of the SEVIRI radiometer, on-board of Meteosat Second Generation satellite. These values were compared with CTBTs calculated using the RTTOV-8 (Proceedings of the Fourteenth International TOVS Study Conference Conference; Beijing, 2005) radiative transfer model and BOLAM water vapour, temperature and hydrometeor profiles. The percentage cloud cover with cloud top temperatures less than 230 K together with ECMWF winds at 250 hPa are shown in Fig. 6. The figure shows the regions of greater convective activity and the TEJ that transports the air masses uplifted by deep convection toward West Africa. Figure 4 shows the percentage of cloud cover calculated from the BOLAM model for the same period. The model reproduces reasonably well the structure and intensity of convective activity. The meridional position of ITCZ in West Africa is displaced northward in the model by about 5 degrees while its northern extent in Sudan and Chad is well simulated. However, BOLAM simulates less convective activity in Democratic Republic of Congo (Dem. Rep. Congo), Cameroon and Nigeria and overestimates convection in central African Republic, Sudan and Chad.

Figure 7 shows the time evolution of tracer profiles averaged over three different areas highlighted in Fig. 4. In these and subsequent figures we only display CO tracers which are 20 days old or younger based on estimates of the chemical of CO lifetime in the lower tropical troposphere (Mauzerall et al., 1998). Area A1 is located just to the north of the emission region and area A2 is located further north. Note that results are not shown below 900 hPa over these regions due to the presence of mountains. Area A3 is located in the region where the aircraft observed the polluted plumes on 13 Au-

ACPD
9, 17385–17427, 2009

gust. Significant tracer arrives in A1 and A2 in the mid-troposphere starting on 17 July in the region A1, and later from 22 July in A2. There is significant periodicity in the modelled tracer transport which depends on the daily position of fires and the intensity of the low level winds. Three episodes of high BB tracer concentrations are visible in A1 in the lower troposphere. The one between 3–11 August 2006 corresponds reasonably well with the break phase of the AEJ-S described by Mari et al. (2008) when pollutants build up over the continent even if the model has higher concentrations for longer over this region. Injection into the UT is also episodic and depends on the position of convective activity relative to the availability of pollutants (tracer) at lower altitudes. There is a clear increase in MT and UT tracer after the 5 August, especially in A2 where the convection is located (see Fig. 6).

At mid-levels (around 650 hPa) over West Africa enhancements in A3 tracer concentration are seen between 27–29 July, 2–5 August and after 14 August. In the UT tracer arrives, albeit with low values on around 1 August with a more intense peak after the 14 August. This later enhancement corresponds well with the plume location measured by the M55 even if the modelled plume arrives 1 day later. The plume is quite dispersed in the vertical but this may be realistic since the DF-20 may have also sampled a BB plume in the UT around 11 km (see Sect. 2).

The ratio of tracer in the MT versus UT can be estimated using observed CO_2 enhancements above background in both plumes and compared with results from the BOLAM model. Enhancements based on measurements of about 11 ppmv and 4 ppmv can be estimated for the MT and UT plumes, respectively (see Figs. 2 and 3) giving a ratio of around 36%. Taking into account the slight delay in higher concentrations reaching the measurement location we use model results on the 14 August to estimate the modelled ratio of UT (200 hPa) to MT (650 hPa) tracer. We derive a mean daily value over a region spanning from -10° W and 10° E and from -420° S to 20° N of 34% and an average value of 36% relative from 13 to 15 August. This agrees very well with the UT to MT ratio based on CO_2 measurements. Comparison with figures displayed in Mari et al. (2008) suggests a lower fraction transported into the upper troposphere

ACPD
9, 17385–17427, 2009

(5–20%) based on FLEXPART driven with ECMWF winds. These results suggest that the BOLAM model has a more effective convective transport, in better agreement with the measurements, for this case.

Since we emitted one tracer per day the results can also be used to estimate the time since emission as a function of altitude. Results over A3 are shown in Fig. 7 averaged over the whole simulation period. The time for tracer to arrive over West Africa with maximum modelled concentrations in the UT (14 August) at 200 hPa is 14 to 15 days whereas the MT plume takes between 16 to 17 days. The transit time between arrival at the measurement location and leaving the emission region was also estimated using mean windspeeds at different altitudes. We derive a transit time of 4–5 days for the MT plume and 1–2 days for the UT plume. This is faster than the 8 days reported by Sauvage et al. (2005). However, this was a climatological (1997–2003) analysis of MOZAIC profile data and could be due to differences in windspeeds between different years. Our results suggest that this transport can be much faster in certain cases.

Examination of tracer concentrations at different altitudes also shows that the MT and UT BB tracer have different origins. During the break phase (e.g. 3–11 August in the model) what becomes UT tracer is uplifted by wet convection in north-western Dem. Rep. Congo and Central Africa Republic (see Fig. 8, upper panels). The MT tracer is transported into the mid-troposphere south of the equator between 10° and 23° S, where wet convection is absent according to the model and less intense according to the satellite cloud measurements (see Figs. 6 and 4). Then it is transported vertically by both dry convection and the baroclinic cell previously described by Sauvage et al. (2005). The MT tracer is also much closer to the BB emission region or even coincident with it (see Fig. 8, upper left panel) compared to the UT tracer which has to be transported to the north-east before being uplifted by deep convection. This results in MT air masses being much richer in BB pollutants compared to UT air masses close to the source region and also downwind over West Africa. (see Fig. 8 for 15 August). These results may explain the significant differences in trace gas concentrations observed in the MT and UT plumes. It also appears that the MT plume is less dispersed

ACPD
9, 17385–17427, 2009

than the UT plume which has been subject to more rapid transport and dispersion by the TEJ (as shown by the different transit times discussed earlier). Washout of soluble species, as well as LiNOx emissions associated with deep convective transport are also likely to have influenced UT trace gas and aerosol concentrations.

Interestingly, the model also simulates significant tracer concentrations up to 200 hPa as far north as 13 N, around the 4/5 August (not shown) and from 11–15 August (Fig. 8). These results suggest that BB emissions could have influenced the chemical composition in the upper troposphere and lower TTL over a larger area than just the southern part of West Africa (as also suggested by Law et al., in preparation, 2009).

In summary, the modelled tracer results support the hypothesis of direct mid-troposphere transport of BB plumes from Central Africa to the southern coast of West Africa. These plumes contain high levels of pollutants probably due to the time spent in the vicinity of the emission regions. We also show that BB pollutants transported further north can be uplifted into the UT and transported westward to the measurement region over West Africa.

4 Ozone production in plumes transported downwind of West Africa

In this section we address the question about whether these plumes continue to produce O_3 downwind from where the measurements were taken. These simulations provide an estimate of changes in O_3 concentrations in these BB plumes during long range transport downwind from African continent. A photochemical model, CiTTyCAT (see Evans et al. (2000); Real et al. (2007) for details) was run along forward trajectories calculated from the location of the BB measurements (MT and UT) using the FLEXTRA model (Stohl et al., 1995) run with ECMWF windfields. The photochemical model was initialised with mean concentrations of available measurements and run forwards for 10 days (see Fig. 9). The MT plume was transported over the southern Atlantic Ocean where it was subject to slow descent before reaching the South American east coast. The UT plume was also transported over ocean where it recirculated back

to the central African coast either in the UT or descending into the MT. Simulations of the chemical fate of both plumes were carried out including diagnosis of chemistry versus mixing effects and the impact of aerosols on photolysis rates.

4.1 Chemical fate of the MT plume

4.1.1 Model set-up

On 13 August 2006, the B-146 sampled the lower part of the plume followed, 3 h later by the DF-20 sampled its upper part. Since these plumes have very similar origin they can be combined to provide mean values to initialise the model MT plume simulations (see Table 1). The forward trajectories show a similar pathway so the model was run along a trajectory representative of the plume transport. Temperature and water vapour from ECMWF along this trajectory were used in the simulations. Three runs were conducted: chemistry-only (Run-CHEM), chemistry plus impact of aerosols on photolysis rates (Run-AER) and chemistry plus aerosols plus mixing/dilution of the plume (Run-MIX). To simulate aerosol impacts on photolysis rates, the FAST-J scheme (Wild et al., 2000) was used (see Real et al. (2007) for details). This scheme requires information about the aerosol optical depth (AOD) of the aerosol layer and aerosol optical properties (AOPs). Refractive indices (RI=1.54−0.078) and aerosol size distributions were taken from measurements made in aged BB plumes from a South African fire (Haywood et al., 2003) and used to calculate AOP using a Mie code (Mishchenko et al., 1999). The 550 nm AOD was retrieved from MODIS satellite measurements (Tanré et al., 1997; Remer et al., 2005) which passed over the Gulf of Guinea on 13 August, and over South Atlantic 7 days later. The collocated CALIPSO lidar data (Winker et al., 2003) clearly show that the main AOD contribution is due to the presence of an aerosol leyer between 4 and 6 km on 13 August and also on 20 August albeit less intense (see Fig. 10). MODIS Aqua aerosol level 2 products version 5 (MYD04) and CALIPSO level 1 version 2 data (532 nm total attenuated backscatter) were used in this analysis. An AOD of 0.9 on 13 August and 0.3 on 20 August were estimated for the aerosol layer.

ACPD
9, 17385–17427, 2009

Therefore, in Run-AER the AOD was allowed to decrease linearly for the first 7 days and then held constant at 0.3.

The dilution of trace gas concentrations in the MT plume were simulated as an exponential decay toward background concentrations with prescribed mixing rates (Evans et al., 2000) based on measurements as far as possible. Observed changes in AOD were used to estimate a mixing rate of 6.4 days, assuming no physical changes during transport and zero background. ECMWF analsyes do not show any precipitation along the trajectory. This mixing rate compares well with values estimated by Real et al. (2007) at mid-latitudes in the free troposphere under meteorological conditions dominated by large-scale advection, as is also the case for the MT plume. For background concentrations measurement taken between 4–8 km during the TRACE-A campaign over the Southern Atlantic and reported in Jacob et al. (1996) were used (see Table 1).

4.1.2 Results

Changes in simulated MT plume concentrations during 10 days are shown in Fig. 11 for Run-CHEM (black continuous line), Run-AER (red dashed line) and Run-MIX (blue dotted line). Run-AER simulates lower O_3 and higher CO than Run-CHEM and Run-MIX generally produces lower concentrations than Run-AER due to mixing with cleaner air masses. Mixing has less impact on more reactive species such as NO_x and also, PAN which is mainly influenced by temperature-driven decomposition.

Net O_3 production (NPO_3) simulated along the trajectory is shown in Fig. 12 together with O_3 production and loss terms. In Run-CHEM, the plume exhibits mean NPO_3 of about 4.7 ppbv/day during the first 4 days and slow net loss (−0.7 ppbv/day) during the last 6 days. This translates into a mean NPO_3 rate of 1.7 ppbv/day over 10 days. The mean NPO_3 in Run-AER is only slightly lower compared to Run-CHEM (1.6 ppbv/day or 6% reduction). However, there is a −25% reduction during the first few days when there is net O_3 production and a net incerease of NPO_3 during the last 6 days when there is net O_3 loss. Aersols have the effect of reducing the photolysis rates of both NO_2 and O_3 and therefore O_3 production and O_3 destruction, respectively. Thus, as

ACPD
9, 17385–17427, 2009

already discussed in Real et al. (2007), when an air mass is in an O_3 destruction regime aerosols reduce the destruction more than the production leading to less O_3 destruction overall. In an O_3 production regime, the production is reduced more than the destruction. In Run-MIX the mean NPO_3 is larger (2.6 ppbv/day) than without mixing. In this run, mean concentrations of O_3 precursors, like VOC, decrease leading to a decrease in O_3 production. However, O_3 itself also strongly decreases due to mixing with clean air masses leading to a larger reduction in O_3 destruction compared to O_3 production.

In the 3 simulations strong O_3 production is maintained by two processes: PAN decomposition during the subsidence of the plume due to increase of the temperature, and HNO_3 photolysis. Both processes lead to NO_2 release followed by photolysis to produce O_3. Sensitivity runs with no PAN decomposition and no HNO_3 photolysis show that these processes contribute almost equally to NPO_3 in the plume. Removal of each process leads to a NPO_3 reduction of almost 80% in each case. PAN has already been shown to play a important role on tropospheric O_3 production far from source regions (Heald et al., 2004; Real et al., 2007) in the case when polluted air masses transported in the free tropsophere descend, releasing NO_x. In the case of plume formation in the lower troposphere, HNO_3 is formed preferentially to PAN and during long-range transport in the lower troposphere (above the boundary layer) in the absence of washout, NPO_3 is a balance between HNO_3 photolysis maintaining NO_x and O_3 production and O_3 destruction by water vapour (Neuman et al., 2006; Real et al., 2008). In the BB case examined here a combination of PAN decomposition and HNO_3 control photochemical O_3 production.

Another interesting feature of this plume is its oxidising capacity. Mean OH values 3.1×10^6 mol cm^{-3} are simulated in Run-MIX, peaking up to 13×10^6 mol cm^{-3}. This leads to 33% reduction in CO over 10 days. Considering a CO background around 100 ppbv, this is equivalent to a CO chemical life-time of about 15 days. This is slightly lower than the CO lifetime of 20 days estimated in tropical lower troposphere based on TRACE-A data by Mauzerall et al. (1998). NPO_3 rates from Run-MIX (2.6 ppbv/day

ACPD
9, 17385–17427, 2009

on average) can be compared with previous estimates of photochemical O_3 production rates in BB plumes transported over the southern Atlantic Ocean. For example, analysis of TRACE-A plumes showed positive O_3 production near source regions followed by either negative or null O_3 production during 5 days downwind (Mauzerall et al., 1998). Chatfield et al. (1996) also found using a 2-D modelisation than O_3 in BB plumes transported over the Atlantic was "cooked then mixed": i.e. produced close to the emissions and then transported and mixed. We calculate an NPO_3 of about 5 ppbv/day during the first 4 days of transport downwind from West Africa even when mixing is taken into account. These results suggest that this plume is still photochemically active far from source emission due to NO_x recycling.

Net O_3 production can also be compared with O_3 budgets estimated over the southern Atlantic. Using a photochemical box model forced with observations, Jacob et al. (1996) estimated a NPO_3 of around −0.7 ppbv/day between 0 to 4 km and 0.3 ppbv/day between 4 and 8 km against 1.5 ppbv/day in the boundary layer and 3 ppbv/day through most of the troposphere in Moxim and Levy (2000). Our simulations suggest that BB plumes transported downwind from Central Africa are still capable of maintaining O_3 levels of around 80 ppbv which are well above background levels of 40–60 ppbv observed by ozonesondes at Cotonou, Benin on the south coast of West African (Thouret et al., in preparation, 2009) or 20 to 50 ppbv observed downwind over the central Atlantic in the lower-mid troposphere (Jenkins et al., 2008).

4.2 Chemical fate of the UT plume

4.2.1 Model set-up

For the UT plume, two runs were performed with chemistry-only (Run-CHEM) and chemistry plus mixing (Run-MIX). No simulation including aerosol impact on photolysis rates were performed because (a) the aircraft only measured part of the plume during the dive making it difficult to estimate the real vertical dimension of the plume and its AOD and (b) aerosol concentrations were lower than for the MT plume possibly due to

ACPD
9, 17385–17427, 2009

a less polluted UT plume or washout so any aerosol impacts are likely to have been smaller. Fewer trace gases measurements were made by the M55 on 13 August which can be used to initialise the plume, namely O_3, NO_y, NO, and CO_2 (see Fig. 3) making it necessary to estimate other species (VOCs, CO, missing NO_y components). This means that the results presented here are not as well constrained as the MT case and provide an initial estimate of NPO_3 in BB in the UT.

In order to estimate initial values, measurements from the MT plumes sampled by the DF-20 and B-146 were used. Assuming plumes underwent the same chemical transformations during transport from BB emission region, the fraction $\Delta Species/\Delta CO_2$ (where Δ is the difference between concentration in the plume and in the background) should be approximately conserved. According to Sect. 3, the plumes have approximately the same age so the level of oxidation in both plumes may not have been very different leading to small differences in CO and VOC lifetimes. By using MT $\Delta CO/\Delta CO_2$ and $\Delta VOC/\Delta CO_2$ to obtain a UT ΔCO and ΔVOC, CO and VOC concentrations in the UT plume were derived. On the other hand, $\Delta NO_y/\Delta CO_2$ is not conserved between plumes and this ratio in the MT plume is much higher than the UT plume (500 pptv/ppmv versus 25 pptv/ppmv). This is probably due to the fact that the UT air mass passed through a convective system with likely loss of HNO_3 (and other soluble gases and aerosols) by washout. Removal of HNO_3 by precipitation may also explain the high NO/NO_y fraction measured in the UT plume compared to the MT plume. LiNOx may also explain this high NO/NO_y fraction but this does not explain the low UT $\Delta NO_y/\Delta CO_2$. Moreover NO in the UT plume is only slightly above mean NO measured by the M55 at that altitude during the campaign and we expect a stronger NO signal from this source. Using DF-20 data, Schalger et al. (in preparation, 2009) estimated NO_x:NO_y ratios of 0.3 to 0.5 in plumes recently influenced by LiNOx and ratios of 0.1–0.2 in plumes 2–3 days old. Therefore, with a NO_x:NO_y ratios around 0.2, LiNOx influence on the UT plume studied here cannot be completely excluded. Therefore, in order to estimate NO_y partitionning in the UT plume, $\Delta PAN/\Delta CO_2$ in the MT was used to derive UT PAN levels, NO_2 levels were estimated using modelled NO_2/NO ratios at steady state,

ACPD
9, 17385–17427, 2009

and the rest of measured NO_y (NO_y – PAN – NO – NO_2) was attributed to HNO_3. All measured and estimated values used to initialise the runs are reported Table 2. Background concentrations were estimated using M55 measurements (CO, CO_2, NO, NO_y, O_3) taken during the whole campaign and by using typical values of tropical UT air masses (TRACE-A measurements) for VOC and NO_y partitioning (Jacob et al., 1996) (see Table 2).

In order to evaluate the mixing time to background for the UT plume we used the BOLAM tracer results at 200 hPa where, as mentioned previously, 32 daily tracers were used to represent the day to day transport of CO BB emissions. Three days were selected when there was injection of tracer at 200 hPa over Eastern/Central Africa followed by decay and no new injection for several days afterwards. Using the hypothesis of an exponential decrease of the concentration toward a background value, a mixing time of 6 to 9 days was calculated using the linear regression of the logarithm of the maximum tracer concentration in the centre of the uplifted (model) plume as a function of time. Therefore, in Run-MIX we estimated a mixing timescale of 7 days.

4.2.2 Results

Results for RUN-CHEM are shown Fig. 13. As shown in Sect. 3, the UT plume is more diluted than the MT plume, and therefore O_3 precursors concentrations are lower. However, NPO_3 is only slightly smaller with a mean value over 10 days of 1.4 ppbv/day compared to 1.6 ppbv/day for the MT plume (chemistry only). In fact both photochemical production and destruction of O_3 are smaller than in the MT plume (about 10% of the MT values). Simulated O_3 concentrations after 10 days are about 72 ppbv in this chemistry only run.

Inclusion of mixing leads to decreases in O_3 concentrations to around 60 ppbv whereas CO concentrations decrease by about 35 ppbv. Mean O_3 net production only slightly decreases to 1.3 ppbv/day thus maintaining O_3 levels despite mixing with lower background concentrations. Therefore, the mean NPO_3 for the UT plume is about half that for the MT plume. Our results compare well with previous estimates of O_3 produc-

tion rates in the tropical upper troposphere of 1.0–1.5 ppbv/day based on analysis of aircraft data (Wennberg et al., 1998; Folkins et al., 2002). Jacob et al. (1996); Moxim and Levy (2000) also estimated O_3 production rates of 1.5–2.1 ppbv/day in the UT over the southern Atlantic which are slightly higher than our estimates. Jacob et al. (1996) suggested that this production is due to transport of NO_x in convective systems over Africa followed by O_3 production downwind. According to our study, part of this NO_x may have a BB origin. Also, the M55 may only have sampled the upper part of the plume during the dive over the Gulf of Guinea (see Fig. 1), and, as such, may not have sampled the highest concentrations. This idea is reinforced by MOZAIC data collected at 11 km showing CO concentrations up to 200 ppbv whereas our estimated CO is around 140 ppbv. A less diluted plume would exhibits stronger O_3 production. In addition, Fig. 7 suggests that BB plumes were present in the UT over West Africa during about one third of the period between mid-July and mid-August 2006. Therefore, as well as LiNOx emissions which have already been shown to make an an important contribution to O_3 over West Africa and downwind over the southern Atlantic (Jenkins and Ryu, 2004a; Sauvage et al., 2007), cross-hemispheric transport of BB pollution from Central Africa also represents an important source of O_3 in the upper troposphere over West Africa. Forward trajectories also show that these air masses were recirculated over the Gulf of Guinea back to Central Africa thus reinforcing the idea that BB emissions contribute to O_3 maxima observed over in the UT over this region between the Equator and 20° S.

5 Conclusions

In this study we examined the origin and O_3 production potential of pollutant plumes observed over the southern coast of West Africa during August 2006 summer monsoon. Analysis of results from the BOLAM mesoscale model, including biomass burning CO tracers confirmed that the likely origin of the plumes was from biomass burning emission regions over Central Africa. Model results showed BB pollutants confined over

ACPD
9, 17385–17427, 2009

Central Africa for between 9–10 days (MT plume) and 12–13 days (UT plume) before being transported to the measurement region 4 days (MT plume) and 2 days (UT plume) later. The MT plume originated from regions closer to the fires thereby explaining the significantly higher observed concentrations. The UT plume was transported to the north-east away from the fire emission region and into a region of deep convection over Chad/Sudan where it was uplifted and transported west by the tropical easterly jet. The UT plume may also have been subjected to LiNOx emissions during convective uplift. Tracer calculations were also used to estimate that around 35% of BB CO tracer was transported into the UT relative to the MT which is a higher fraction that previously reported. Our model results agree well with the ratio derived from observed CO_2 enhancements in both plumes.

Net O_3 production downwind from West Africa was evaluated using a photochemical trajectory model initialized with measurements. Results show that the MT plume was still very chemically active during 10 days downwind over the Atlantic Ocean with a mean net O_3 production rate of 2.6 ppbv/day and up to 7 ppbv/day during the first few days. Simulated O_3 in the centre of the plume decreased due to mixing with cleaner background. O_3 production was due to NO_x release from PAN and HNO_3, with an equal contribution from both NO_x reservoirs. Positive net O_3 production was also estimated in the UT plume albeit at a slower rate (1–2 ppbv/day) and taking into account mixing derived from the tracer simulations. In this case, the plume was recirculated around an upper level anticyclone back towards the African continent at 20 S. Our results support the hypothesis that BB plume from Central Africa are contributing to observed O_3 maxima over the southern Atlantic Ocean.

Acknowledgements. Based on a French initiative, AMMA was built by an international scientific group and is currently funded by a large number of agencies, especially from France, the UK, the USA, and Africa. It has been a beneficiary of a major financial contribution from the European Community Sixth Framework Programme (AMMA-EU). Detailed information on scientific coordination and funding is available on the AMMA International website at www.amma-international.org.

The DF-20 campaign was funded partly through AMMA-EU. The M55-Geophysica campaign was funded by AMMA-EU, EC Integrated Project SCOUT-O3 (505390-GOCE-CT-2004), CNRS-INSU, CNES, EUFAR and the M55 aircraft consortium. We would like to thank all the scientists aircraft operators as well as local scientists and representatives in Burkina Faso for their help and support during the planning and execution of the Ouagadougou campaign. We also acknowledge support from the AMMA Operations Centre in Niamey, Niger.

The B-146 campaign was funded in part by AMMA-EU and also through a NERC AMMA-UK consortium grant. We also acknowledge B-146 data provided by the Facility for Airborne Atmospheric Measurements (FAAM) and the British Atmospheric Data Centre (BADC). E. Real acknowledges funding from the AMMA-EU.

The publication of this article is financed by CNRS-INSU.

References

Ancellet, G., Leclair de Bellevue, J., Mari, C., Nedelec, P., Kukui, A., Borbon, A., and Perros, P.: Effects of regional-scale and convective transports on tropospheric ozone chemistry revealed by aircraft observations during the wet season of the AMMA campaign, Atmos. Chem. Phys., 9, 383–411, 2009, http://www.atmos-chem-phys.net/9/383/2009/. 17390, 17392

Andres-Hernandez, M. D., Kartal, D., Reichert, L., Burrows, J. P., Arnek, J. M., Lichtenstern, M., Stock, P., and Schlager, H.: Peroxy radical observations over West Africa during the AMMA 2006 campaign: photochemical activity in the outflow of convective systems, Atmos. Chem. Phys., 9, 3681–3695, 2009, http://www.atmos-chem-phys.net/9/3681/2009/. 17389, 17391

Barret, B., Ricaud, P., Mari, C., Attie, J.-L., Bousserez, N., Josse, B., Flochmoen, E. L., Livesey, N., Massart, S., Peuch, V.-H., Piacentini, A., Sauvage, B., Thouret, V., and Cammas, J.-P.: Transport pathways of CO in the African upper troposphere during the monsoon season: a study based upon the assimilation of spaceborne observations, Atmos. Chem. Phys., 8, 3231–3246, 2008, http://www.atmos-chem-phys.net/8/3231/2008/. 17389

Borrmann, S., et al.: Aerosols in the tropical and subtropical UT/LS: in situ measurements of ultrafine particle abundance and volatility, in preparation, 2009. 17392

Burpee, R. W.: The origin and structure of easterly waves in the lower troposphere of North Africa, JAS, 29, 77–90, 1972. 17393

Buzzi, A. and Foschini, L.: Mesoscale meteorological features associated with heavy precipitation in the southern Alpine region, Meteorologic and Atmospheric Physic, 72, 131–146, 2000. 17394

Cairo, F., et al.: An overview of the SCOUT-O3-AMMA stratospheric aircraft, balloons and sondes campaign in West Africa, August 2006: rationale, roadmap and highlights, in preparation, 2009. 17391

Chatfield, R., Vastano, J. A., Singh, H. B., and Sachse, G.: A general model of how fire emissions and chemistry produce African/oceanic plumes (O3 , CO, PAN, smoke) in TRACE-A, JGR, 101, 24279–24306, 1996. 17389, 17402

Crutzen, P. J. and Andreae, M. O.: Biomass burning in the tropics: Impact on atmospheric chemistry and biogeochemical cycles, Science, 250, 1669–1678, 1990. 17388

Evans, M. J., Shallcross, D. E., Law, K. S., Wild, J. O. F., Simmonds, P. G., Spain, T. G., Berrisford, P., Methven, J., Lewis, A. C., McQuaid, J. B., Pillinge, M. J., Bandyf, B. J., Penkett, S. A., and Pyle, J. A.: Evaluation of a Lagrangian box model using field measurements from EASE (Eastern Atlantic Summer Experiment) 1996, Atmos. Environ., 34, 3843–3863, 2000. 17398, 17400

Fueglistaler, S., Dessler, A. E., Dunkerton, T. J., Folkins, I., Fu, Q., and Mote, P. W.: Tropical tropopause layer, revgeo, 47, RG1004, doi:10.1029/2008RG000267, 2009. 17391

Haywood, J. M., Osborne, S. O., Francis, P. N., Keil, A., Formenti, P., Andreae, M. O., and Kaye, P. H.: The mean physical and optical properties of regional haze dominated by biomass burning aerosol measured from the C-130 aircraft during SAFARI 2000, J. Geophys. Res., 107, D8473, doi:10.1029/2002JD002226, 2003. 17399

Heald, C. L., Jacob, D. J., Fiore, A. M., Emmons, L. K., Gille, J. C., Deeter, M. N., Warner, J.,

Edwards, D. P., Crawford, J. H., Hamlin, A. J., Sachse, G. W., Browell, E. V., Avery, M. A., Vay, S. A., Westberg, D. J., Blake, D. R., Hanwant, B., Sandholm, S. T., Talbot, R. W., and Fuelberg, H. E.: Asian outflow and trans-Pacific transport of carbon monoxide and ozone pollution: An integrated satellite, aircraft, and model perspective., J. Geophys. Res., 108, D4804, doi:10.1029/2003JD003507, 2004. 17401

Jacob, D. J., Heikes, B. G., Fan, S.-M., Logan, J. A., Mauzerall, D. L., Bradshaw, J. D., Singh, H. B., Gregory, G. L., Talbot, R. W., Blake, D. R., W., G., and Sachse: Origin of ozone and NO_x in the tropical troposphere: A photochemical analysis of aircraft observations over the South Atlantic basin, JGR, 101, 24235–24250, 1996. 17389, 17400, 17402, 17404, 17405, 17413, 17414

Janicot, S., Thorncroft, C. D., Ali, A., Asencio, N., Berry, G., Bock, O., Bourles, B., Caniaux, G., Chauvin, F., Deme, A., Kergoat, L., Lafore, J.-P., Lavaysse, C., Lebel, T., Marticorena, B., Mounier, F., Nedelec, P., Redelsperger, J.-L., Ravegnani, F., Reeves, C. E., Roca, R., de Rosnay, P., Schlager, H., Sultan, B., Tomasini, M., Ulanovsky, A., and ACMAD forecasters team: Large-scale overview of the summer monsoon over West Africa during the AMMA field experiment in 2006, Ann. Geophys., 26, 2569–2595, 2008, http://www.ann-geophys.net/26/2569/2008/. 17393

Jenkins, G. S. and Ryu, J.-H.: Space-borne observations link the tropical atlantic ozone maximum and paradox to lightning, Atmos. Chem. Phys., 4, 361-375, 2004a. 17388, 17405

Jenkins, G. S. and Ryu, J.-H.: Linking horizontal and vertical transports of biomass fire emissionsto the tropical Atlantic ozone paradox during the Northern Hemisphere winter season: climatology, Atmos. Chem. Phys., 4, 449–469, 2004b. 17389

Jenkins, G. S., Mohr, K., Morris, V. R., and Arino, O.: The role of convective processes over the Zaire-Congo Basin to the southern hemispheric ozone maximum, JGR, 102, 18963–18980, 1997. 17388

Jenkins, G. S., Camara, M., and Ndiaye, S. A.: Observational evidence of enhanced middle/upper tropospheric ozone via convective processes over the equatorial tropical Atlantic during the summer of 2006, GRL, 35, L12806, doi:10.1029/2008GL0033954, 2008. 17402

Moxim, J. W. and Levy, H.: A model analysis of the tropical South Atlantic Ocean tropospheric ozone maximum: The interaction of transport and chemistry, JGR, 105, 17 393–17 416, 2000. 17402, 17405

Kain, J.: The KainFritsch convective parameterization: An update, J. Appl. Meteorol., 43, 170–181, 2004. 17394

Law, K. S., Cairo, F., Fierli, F., Palazzi, E., Borrmann, S., Schlager, H., Streibel, M., Viciani, S., Ravegnani, F., Volk, M., and Schiller, C.: Air mass origins influencing TTL chemical composition over West Africa during the 2006 summer monsoon, Atmos. Chem. Phys. Discuss., submitted, 2009. 17392

Liousse C., Guillaume, B., Grégoire, J. M., Mallet, M., Galy, C., Pont, V., Solmon, F., Poirson, A., Rosset, R., Serça, D., Mariscal, A., Dungal, L., V. Yoboué, Bedou, X., Konaré, A., Granier, C., Mieville, A., and van Velthoven, P.: Western African Aerosols Modeling with real time biomass burning emission inventories in the frame of AMMA-IDAF program, Atmos. Chem. Phys. Discuss., submitted, 2009. 17394

Malguzzi, P., Grossi, G., Buzzi, A., Ranzi, R., and Buizza, R.: The 1966 century flood in Italy: A meteorological and hydrological revisitation., J. Geophys. Res., 111, D24106, doi:10.1029/2006JD00711, 2006. 17394

Mari, C. H., Cailley, G., Corre, L., Saunois, M., Atti, J. L., Thouret, V., and Stohl, A.: Tracing biomass burning plumes from the Southern Hemisphere during the AMMA 2006 wet season experiment, Atmos. Chem. Phys., 8, 3951–3961, 2008, http://www.atmos-chem-phys.net/8/3951/2008/. 17388, 17393, 17394, 17396

Mauzerall, D. L., Logan, J. A., Jacob, D. J., Anderson, B. E., Blake, D. R., Bradshaw, J. D., Haikes, B., Sachse, G. W., Singh, H., and Talbot, B.: Photochemistry in biomass burning plumes and implications for tropospheric ozone over the tropical South Atlantic, J. Geophys. Res., 103, 8401–8423, 1998. 17389, 17395, 17401, 17402

Mishchenko, M. I., Goegdzhayev, I., Cairns, B., Rossow, W. B., and Lacis, A. A.: Aerosol retrievals over the ocean by use of channels 1 and 2 AVHRR data: sensitivity analysis and preliminary results, Appl. Optics., 38, 7325–7341, 1999. 17399

Neuman, J. A., Parrish, D. D., Trainer, M., Ryerson, T. B., Holloway, J. S., Nowak, J. B., Swanson, A., Flocke, F., Roberts, J. M., Brown, S. S., Stark, H., Sommariva, R., Stohl, A., Peltier, R., Weber, R., Wollny, A. G., Sueper, D. T., Hubler, G., and Fehsenfeld, F. C.: Reactive nitrogen transport and photochemistry in urban plumes over the North Atlantic Ocean, J. Geophys. Res., 111, D23S54, doi:10.1029/2005JD007 010, 2006. 17401

Nicholson, S. E. and Grist, J.: The seasonal evolution of the at- mospheric circulation over West Africa and Equatorial Africa, J. Climate, 16, 1013–1030, 2003.

Park, S., Jimnez, R., Daube, B. C., Pfister, L., Conway, T. J., Gottlieb, E. W., Chow, V. Y., Curran, D. J., Matross, D. M., Bright, A., Atlas, E. L., Bui, T. P., Gao, R.-S., Twohy, C. H., and Wofsy, S. C.: The CO2 tracer clock for the Tropical Tropopause Layer, Atmos. Chem. Phys.,

7, 3989–4000, 2007,
http://www.atmos-chem-phys.net/7/3989/2007/. 17393
Proceedings of the Fourteenth International TOVS Study Conference, in: RTTOV-8 the latest update to the RTTOV model, Beijing, China, t. s. M., 2005. 17391
Real, E., Law, K. S., Wienzierl, B., Fiebig, M., Petzold, A., Wild, O., Methven, J., Arnold, S., Stohl, A., Huntrieser, H., Roiger, A., Schlager, H., Stewart, D., Avery, M., Sachse, G., Browell, E., Ferrare, R., and Blake, D.: Processes influencing ozone levels in Alaskan forest fires plumes during long-range transport over the North Atlantic, J. Geophys. Res., 112, D10S41, doi:10.1029/2006JD007 576, 2007. 17395
Real, E., Law, K. S., Schlager, H., Roiger, A., Huntrieser, H., Methven, J., Cain, M., Holloway, J., Neuman, J. A., Ryerson, T., Flocke, F., de Gouw, J., Atlas, E., Donnelly, S., and Parrish, D.: Lagrangian analysis of low altitude anthropogenic plume processing across the North Atlantic, Atmos. Chem. Phys., 8, 7737–7754, 2008,
http://www.atmos-chem-phys.net/8/7737/2008/. 17398, 17399, 17400, 17401
Remer, L., Kaufman, Y. J., Tanré, D., Mattoo, S., Chu, D. A., Martins, J. V., Li, R. R., Ichoku, C., Levy, R. C., Kleidman, R. G., Eck, T. F., Vermote, E., and Holben, B. N.: The MODIS Aerosol Algorithm, Products, and Validation, J. Atmos. Sci., 62, 947–973, 2005. 17401
17399
Reeves, C. E., Formenti P., Ancellet, J.-L., Attie, J. Bechara, A. Borgon, F., Cairo, H., Coe, F., Fierli, C., Flamant, L., Gomes, C., Lambert, K. S., Law, C., Mari, J., Methven, A., Minikin, J. K., Nielsen, A., Richter, H., Schlager, A., Schwarzenboeck, and Thouret, V.: Chemical characterisation of the troposphere over West Africa during the monsoon period as part of AMMA, Atmos. Chem. Phys. Discuss., to be submitted, 2009. 17390
Sauvage, B., Thouret, V., Cammas, J.-P., Gheusi, F., Athier, G., and Nédélec, P.: Tropospheric ozone over Equatorial Africa: regional aspects from the MOZAIC data, Atmos. Chem. Phys., 5, 311–335, 2005,
http://www.atmos-chem-phys.net/5/311/2005/. 17388, 17397
Sauvage, B., Thouret, V., Thompson, A. M., Witte, J. C., Cammas, J.-P., Nedelec, P., and Athier, G.: Enhanced view of the tropical Atlantic ozone paradox and zonal wave one from the in situ MOZAIC and SHADOZ data, J. Geophys. Res., 111, D01301, doi:10.1029/2005JD006241, 2006. 17388, 17393
Sauvage, B., Martin, R. V., van Donkelaar, A., and Ziemke, J. R.: Quantification of the factors controlling tropical tropospheric ozone and the South Atlantic maximum, J. Geophys. Res.,

112, D11309, doi:10.1029/2006JD008008, 2007. 17389, 17405
Stohl, A., Wotawa, G., Seibert, P., and Kromp-Kolb, H.: Interpolation errors in wind fields as a funcion of spatial and temporal resolution and their impact on different types of kinematic trajectories, J. Appl. Meteorol., 34, 2149–2165, 1995. 17398
Tanré, D., Kaufman, Y., Herman, M., and Mattoo, S.: Remote sensing of aerosol properties over oceans using the MODIS sol EOS spectral radiances, JGR, 102, 16971–16988, 1997. 17399
Thompson, A. M., Pickering, K., McNamara, D. P., Schoeberl, M. R., Hudson, R. D., Kim, J. H., Browell, E. W., Kirchhoff, V. W. J. H., and Nganga, D.: Where did tropospheric ozone over southern Africa and the tropical Atlantic come from in October 1992? Insights from TOMS, GTE TRACE A, and SAFARI 1992, J. Geophys. Res., 108, 101, 24,251–24,278 , 1996. 17388, 17389
Voigt, C., Schlager, H., Roiger, A., Stenke, A., de Reus, M., Borrmann, S., Jensen, E., Schiller, C., Konopka, P., and Sitnikov, N.: Detection of reactive nitrogen containing particles in the tropopause region – evidence for a tropical nitric acid trihydrate (NAT) belt, Atmos. Chem. Phys., 8, 7421–7430, 2008, http://www.atmos-chem-phys.net/8/7421/2008/. 17391
Weller, R., Lilischkis, R., Schrems, O., Neuber, R., and Wessel, S.: Vertical ozone distribution in the marine atmosphere over the central Atlantic Ocean (56° S–50° N), JGR, 101, 1387–1400, 1996. 17388
Wild, O., Zhu, X., and Prather, M. J.: Fast-J: Accurate Simulation of In- and Below- Cloud Photolysis in Tropopsheric Chemical Models, J. Atmos. Chem., 37, 245–282, 2000. 17399

Table 1. Mean concentrations measured in the MT plume by the Bae-146 and the DLR Falcon aircrafts. Concentrations used to initialised the box model calculation are given in the third column. In case both aircrafts measured the same species, the average is calculated. HNO_3 is calculated as the sum: (NO_y – PAN – NO_2 – NO). Background concentrations are taken from Jacob et al. (1996) (4–8 km).

	Bae-146	DLR Falcon	Initialisation	Background concentrations
CO (ppbv)	385	373	379	103
O_3 (ppbv)	108	116	112	69
NO (pptv)	244	196	220	29
NO_2 (pptv)		300	300	50
PAN (pptv)	1200		1200	294
HNO_3 (pptv)			6000	130
NO_y		7720		
C_2H_4 (pptv)	18		18	
C_2H_6 (pptv)	2760		2760	630
C_2H_2 (pptv)	1400		1400	130
C_3H_6 (pptv)	4		4	4
C_4H_10 (pptv)	30		30	
C_5H_12 (pptv)	4		4	
C_6H_6 (pptv)	326		326	21
C_7H_8 (pptv)	10		10	2
Formaldehyde (pptv)	1110		1110	40
Acetaldehyde (pptv)	1030		1030	320
Acetone (pptv)	2010		2010	593
CO_2 (ppmv)		387		376

ACPD
9, 17385–17427, 2009

Table 2. Mean concentrations measured in the UT plume by the M55 aircraft. Concentrations used to initialised the box model calculation are given in the second column (see text for details). Background concentrations are taken from Jacob et al. (1996) (8–12 km).

	M55	Initialisation	Background concentrations
CO (ppbv)		130	75
O_3 (ppbv)	60	60	50
NO (pptv)	220	220	150
NO_2 (pptv)		200	10
PAN (pptv)		330	223
HNO_3 (pptv)		70	59
NO_y	820		
C_2H_4 (pptv)	6	6	9
C_2H_6 (pptv)	1000	1000	670
C_2H_2 (pptv)	490	490	110
C_3H_6 (pptv)	1	1	4
C_4H_10 (pptv)	10	10	
C_5H_12 (pptv)	1	1	
C_6H_6 (pptv)	100	100	15
C_7H_8 (pptv)	3	3	2
Formaldehyde (pptv)	400	400	40
Acetone (pptv)	1070	1070	650
CO_2 (ppmv)	380		376

ACPD
9, 17385–17427, 2009

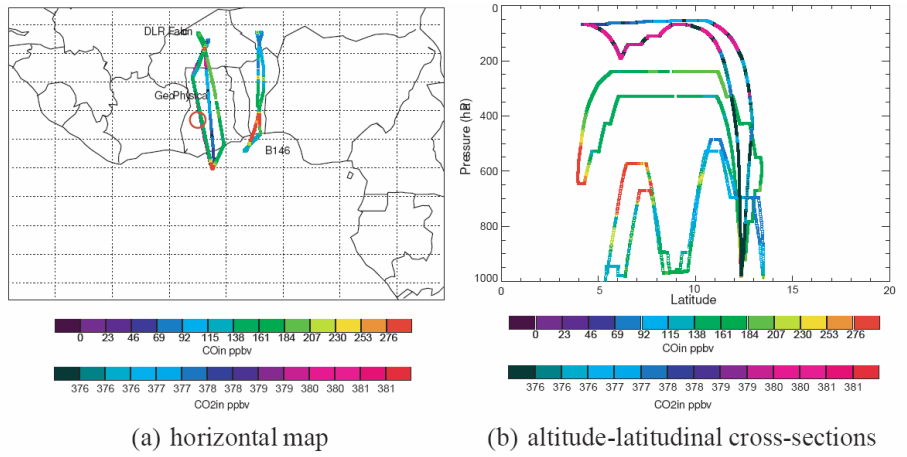

(a) horizontal map (b) altitude-latitudinal cross-sections

Fig. 1. Flight path for 13 August 2006 flight. Colour scales represent the CO concentrations from the DF-20 and the B-146 and CO_2 concentrations for the M55 aircraft. See text for details.

ACPD
9, 17385–17427, 2009

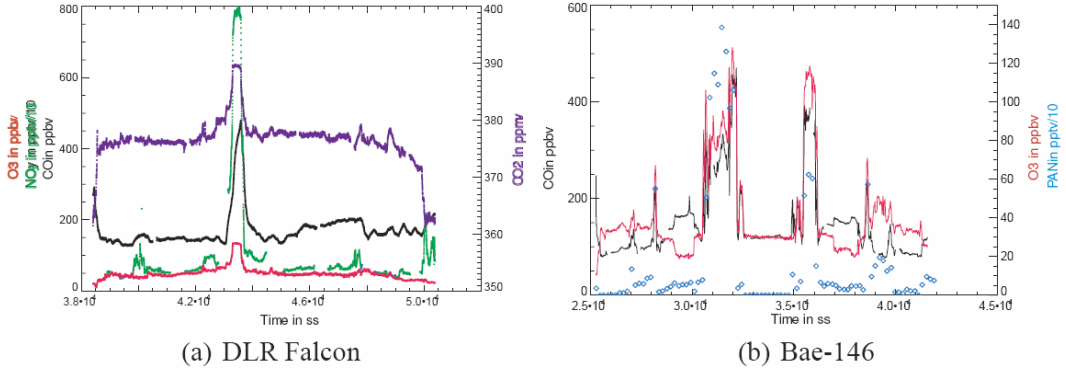

Fig. 2. Measurements taken on 13 August 2006 by the DLR Falcon aircraft (left hand) and the Bae-146 (right hand).

ACPD
9, 17385–17427, 2009

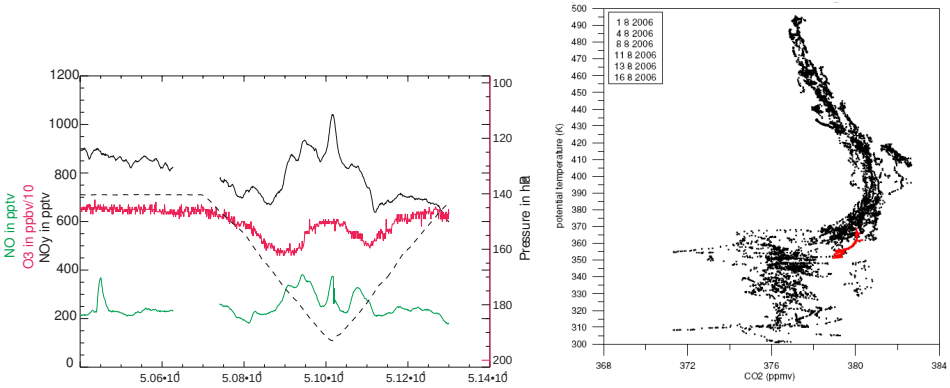

(a) NO, NO_y, O_3 (b) CO_2

Fig. 3. Right hand figure: Measurements of NO, NO_y and O_3 taken on 13 August 2006 by the GeoPhysica. Left hand figure: Measurements of CO_2 taken during the whole campaign, CO_2 measured during the dive on the 13 August is highlighted in red.

ACPD
9, 17385–17427, 2009

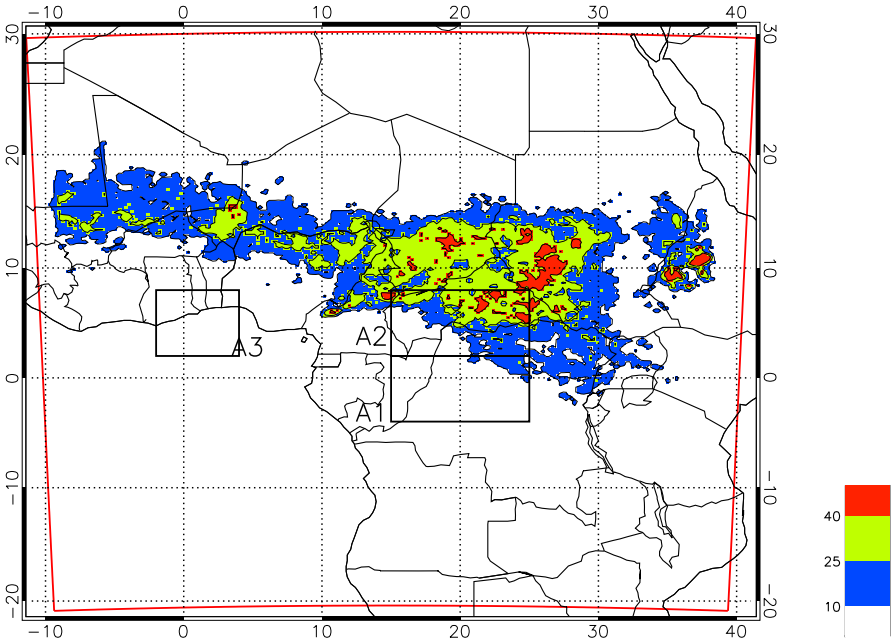

Fig. 4. Percentage of cloud cover for model-derived cloud top brightness temperature less than 230 K. Cloud Percentage is relative to the period 15 July–15 August. Black squares indicate the averaging area used in Fig. 7. Red box indicates the BOLAM model domain.

ACPD
9, 17385–17427, 2009

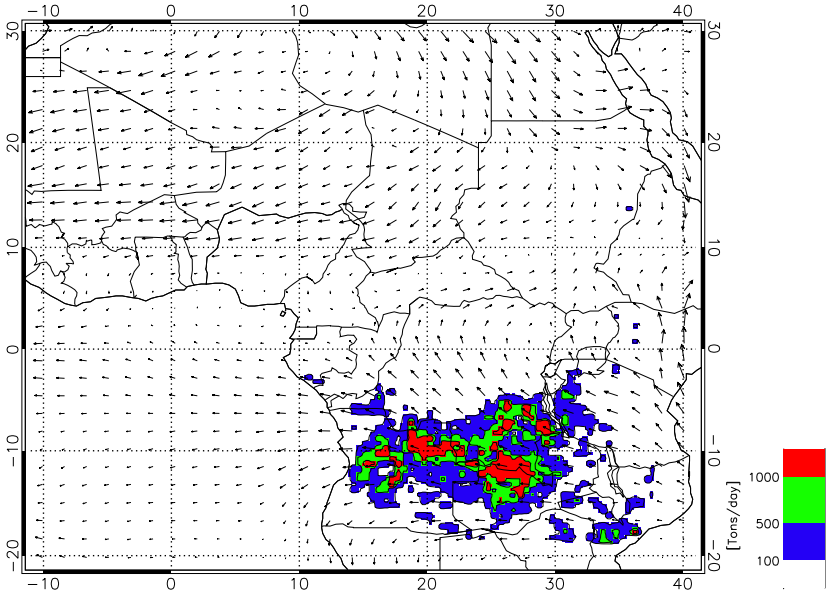

Fig. 5. CO flux averaged between 15 July and 15 August. Thin arrows are ECMWF wind field averaged between 15 July and 15 August at 750 hPa.

ACPD

9, 17385–17427, 2009

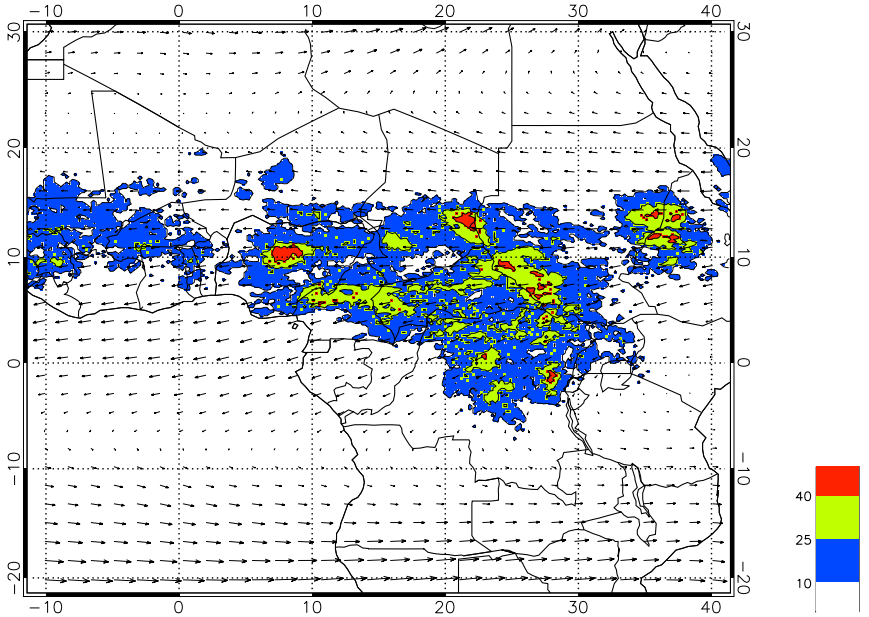

Fig. 6. Percentage of cloud cover for cloud top brightness temperature less than 230 K, evaluated from MSG-SEVIRI radiometer. Percentage is relative to the period 15 July–15 August. Thin arrows are ECMWF wind field at 250 hPa averaged over the same period.

ACPD
9, 17385–17427, 2009

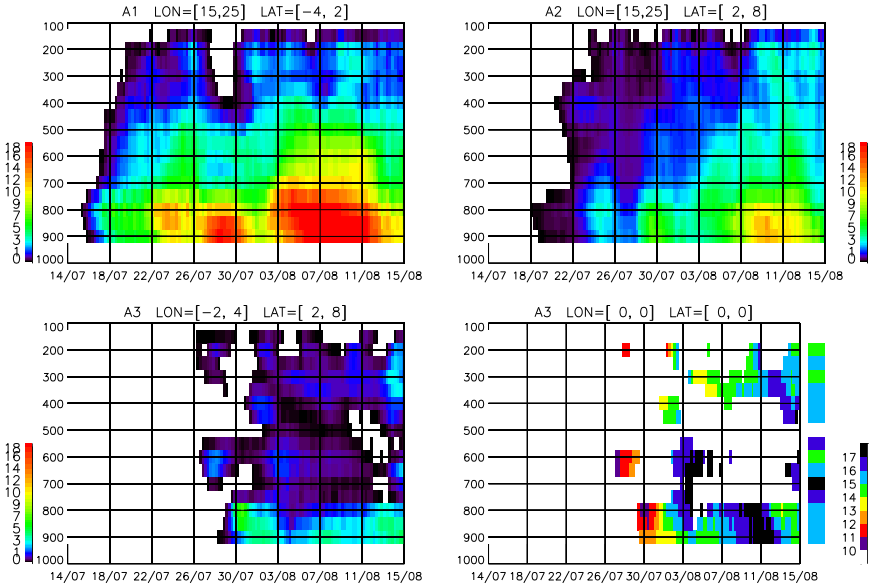

Fig. 7. Hovmoller plot of Tracer concentration profiles (top and bottom left panels). Limits of the three averaging areas are reported on the top of each panels (see also Fig. 4). Tracer travel time for averaging area A3 (Bottom right panel).

ACPD
9, 17385–17427, 2009

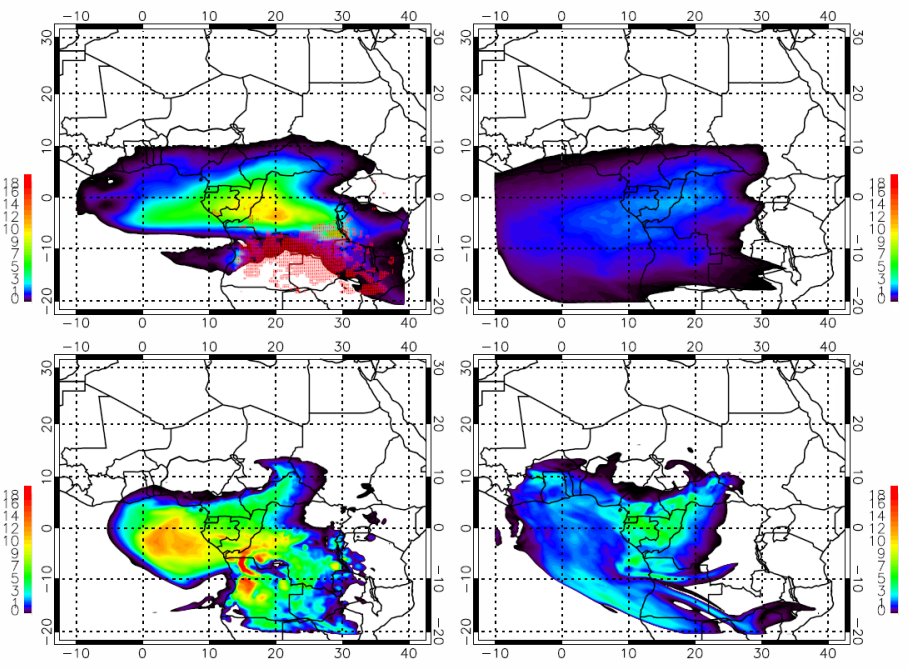

Fig. 8. Tracer concentrations on 9 August 18:00 UTC at 650 hPa and 200 hPa (respectively upper left and right panel), 15 August 18:00 UTC at 650 hPa and 200 hPa (respectively bottom left and right panel).

ACPD

9, 17385–17427, 2009

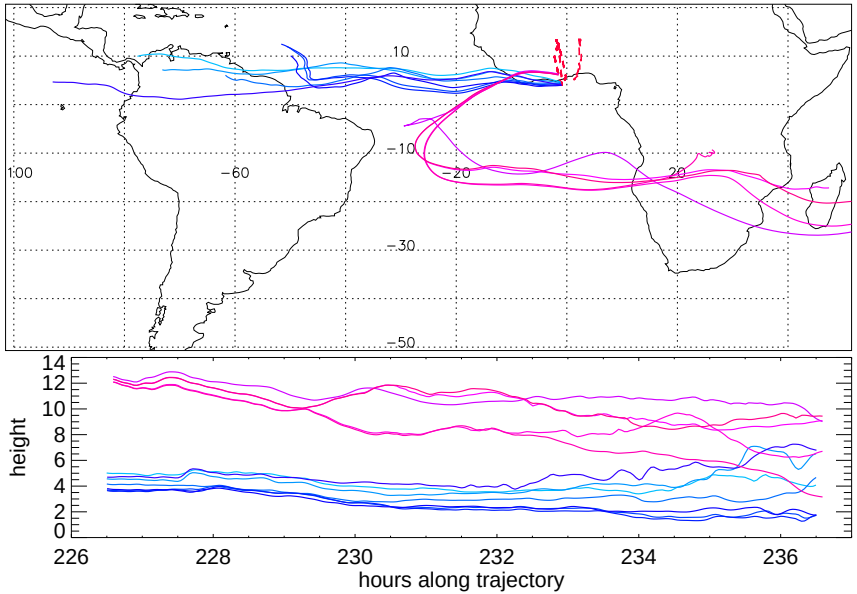

Fig. 9. 10 days simulated forward trajectories initialised from the MT plume (blue lines) and the UT plume (mink lines). Flight tracks of the DLR Falcon, the BAe-146 and the GeoPhysica aircrafts are represented as red dashed lines.

ACPD
9, 17385–17427, 2009

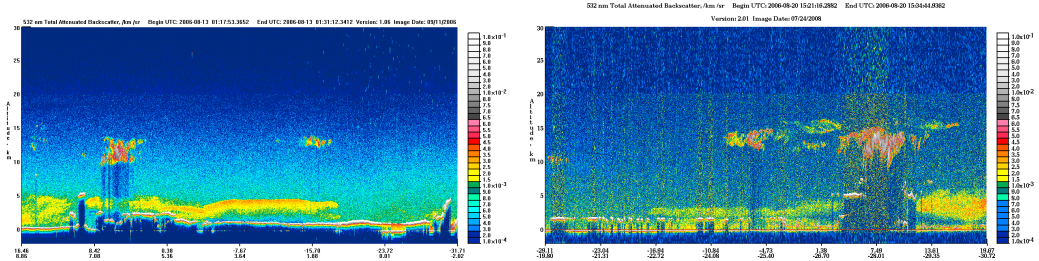

(a) 13 August (b) 20 August

Fig. 10. CALIPSO images during the paths of 13 August over the Gulf of Guinea (right hand) and over the SAO on 20 August (left hand). Plumes with high concentrations of aerosols are visible between 2 and 5 km.

ACPD

9, 17385–17427, 2009

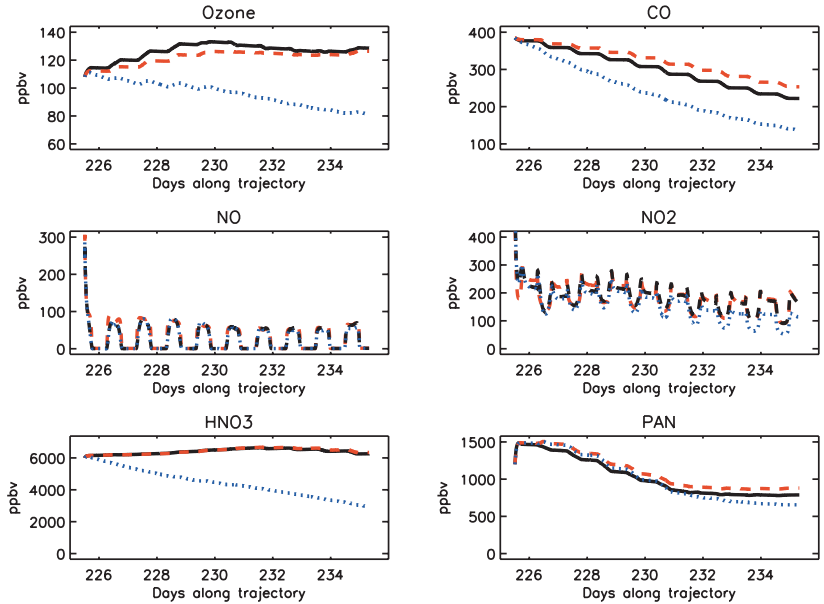

Fig. 11. Simulated concentrations in the MT plume for case RUN-CHEM (black lines), RUN-AEROSOL (red lines) and RUN-MIXING (blue lines).

ACPD
9, 17385–17427, 2009

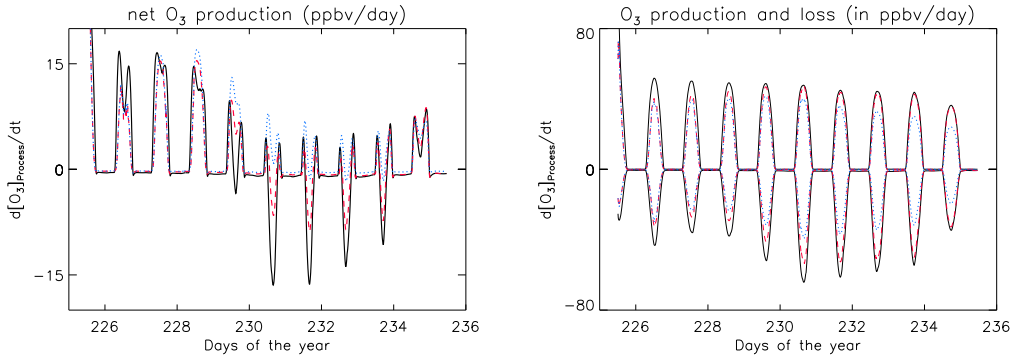

(a) O_3 net production

(b) O_3 production and loss

Fig. 12. 10 days simulated net O_3 production (left hand) and simulated production and destruction terms (right hand) in the MT plume.

ACPD

9, 17385–17427, 2009

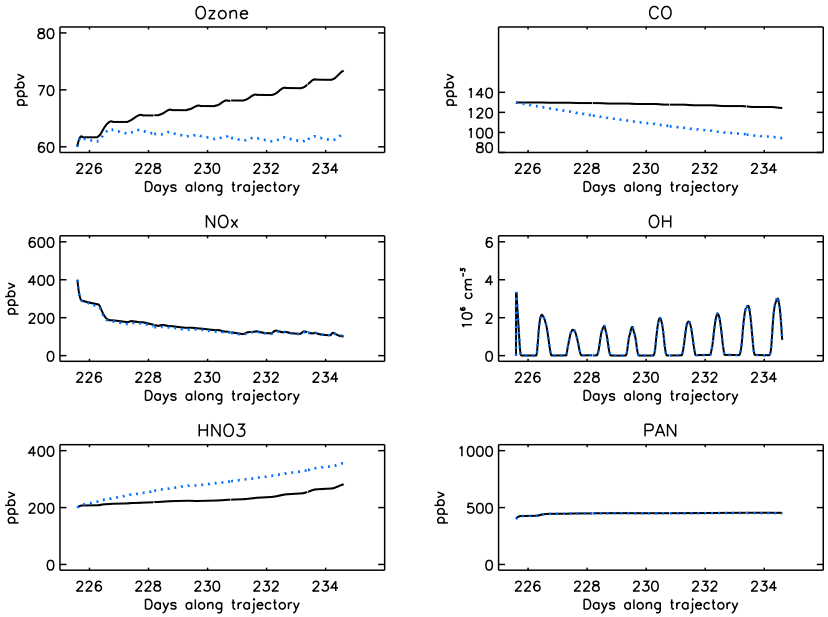

Fig. 13. 10 days simulated concentrations in the UT plume in the case RUN-CHEM (black line) and RUN-MIXING (blue lines).

ACPD
9, 17385–17427, 2009